Journal of Research Updates in Polymer Science, **2023**, *12*, 171-179

Ether Bond Formation in Waste Biomass–Derived, Value-Added Technical Hardwood Kraft Lignin Using Glycolic Acid

Saman Ghahri and Byung-Dae Park*

Department of Wood and Paper Science, Kyungpook National University, Daegu, 41566, Republic of Korea

Abstract: Ether bond formation in technical hardwood kraft lignin (THKL) by crosslinking using glycolic acid was investigated for bio-adhesive applications. Industrial hardwood kraft black liquor was used to extract the THKL utilized by acidification. Chemical and thermal properties of the THKL with and without crosslinking were analyzed by Fourier transform infrared (FTIR) spectroscopy, solid-state ^{13}C cross-polarization/magic angle spinning nuclear magnetic resonance (^{13}C CP/MAS NMR) spectroscopy, X-ray photoelectron spectroscopy (XPS), gel permeation chromatography (GPC), differential scanning calorimetry (DSC), and thermogravimetric analysis (TGA). FTIR results revealed a new peak corresponding to the ether bond and hemiacetal formation due to crosslinking at 1075 cm^{-1} and 1324 cm^{-1}. ^{13}C CP/MAS NMR spectra revealed the presence of a higher number of ether bonds due to the reduced aromatic and aliphatic hydroxyl groups in THKL and new bonds formed at 62-64 ppm and 168-191 ppm due to crosslinking. XPS results revealed that new bonds were formed between glycolic acid and THKL, leading to increased atomic oxygen percentage and carbon–oxygen bonds in crosslinked THKL detected by peak intensity changes at 287.7 and 288.8 related to O–C–O and O–C=O. Also, the oxygen content increased from 14.88% to 31.76% due to bond formation. GPC confirmed a higher molecular weight and broader molecular-weight distribution of THKL. DSC and TGA curves of crosslinked THKL revealed exothermic behavior, high thermal stability, and low thermal degradation rate. Owing to a significant amount of kraft black liquor being generated by wood pulp industries and attractive chemical properties of THKL, THKL demonstrates promise as a raw material to produce green, sustainable bio-adhesives via the crosslinking of its different hydroxyl groups using glycolic acid.

Keywords: Waste black liquor, hardwood kraft lignin, bio-materials, bio-adhesives, eco-friendly products, sustainability.

1. INTRODUCTION

Lignin is the second most abundant biopolymer in nature. It functions as a polysaccharide binder in plant cell walls, assembling and shielding cellulose and hemicellulose chains while endowing hydrophobicity and strength to the lignocellulosic matrix. Hardwood and softwood species comprise specific amounts of lignin in their wood structures. Based on the manufacturing unit used for preparation, lignin is classified into three types: p-hydroxyphenyl (H) lignin, guaiacyl (G) lignin, and syringyl (S) lignin, which are prepared using monolignols p-coumaryl, coniferyl, and sinapyl alcohols, respectively [1]. Furthermore, lignin can be classified into two main groups: natural lignin, which is directly extracted from lignocellulosic materials, and technical lignin, which is extracted from waste generated during chemical wood pulping. Currently, technical lignin is primarily produced by wood pulping industries [2]. Based on wood pulping methods used, technical lignin is categorized into kraft lignin, soda lignin, lignosulfonate, and organosolv lignin. Owing to different reaction chemistry of wood pulping processes, technical lignin exhibits specific properties, which are different from those of natural lignin. In addition, the chemical and molecular characteristics of different types of technical lignin are different.

Information regarding the chemical reactions occurring during kraft pulping is still limited. Nevertheless, some studies have investigated the mechanisms as well as bonds formed during kraft pulping by nuclear magnetic resonance (NMR) spectroscopy to understand the chemical reactions occurring during delignification using kraft pulping methods. Results revealed that the retro-Aldol reaction during the kraft pulping process causes the cleavage of side chains, affording guaiacol radicals, especially when using lignin with low molar-mass fractions. After radical coupling, a highly condensed aromatic conjugate (e.g., 1–1′, 4–O–5′, 5–5′, and 1–5′) is formed to stabilize these fractions under alkaline conditions [3, 4]. Generally, owing to its complex structure in different lignocellulosic plants, high molecular-weight dispersity, and low chemical reactivity, natural lignin poses some challenges for use as raw materials. Meanwhile, owing to intense chemical treatment during pulping, technical lignin is more complicated. Studies have estimated that the maximum production output of kraft lignin was approached 150 kt/y, but around 99% of total black liquor still was burned in concentrated form [5].

---

*Address correspondence to this author at the Department of Wood and Paper Science, Kyungpook National University, Daegu, 41566, Republic of Korea; Tel: +82-53-950-5797; Fax: +82-53-950-6751; E-mail: byungdae@knu.ac.kr

E-ISSN: 1929-5995/23

Nevertheless, only approximately 1% of technical lignin is recovered for utilization in various applications.

Currently, owing to the restrictions on formaldehyde emissions during the production of traditional synthetic wood adhesives, e.g., urea–formaldehyde and phenol–formaldehyde thermoset resins, identifying a bio-adhesive with properties similar to the synthetic ones is a priority for related industries. Owing to its natural polymeric structure, abundance, and cost effectiveness (extracted from waste), technical lignin is an excellent candidate material for bio-adhesive production to replace formalin-based wood adhesives. This valuable raw material poses some serious challenges and issues such as broad chemical variation, complex structure, high molecular-weight dispersity, high heterogeneity, and low reactivity. The low reactivity of lignin prevents its chemical bonding during production.

Herein, means for enhancing the reactivity of technical hardwood kraft lignin (THKL) using eco-friendly materials to produce bio-based wood adhesives without using formaldehyde were investigated. For this purpose, THKL was isolated from industrial waste black liquor by acidification. To improve its reactivity, a 40% glyoxal solution was used to form a crosslinked network. For the first time, different aspects of aromatic and aliphatic –OH reactivity of THKL during crosslinking were considered.

2. MATERIALS AND METHODS

Industrial mixed hardwood kraft black liquor with a solid content of ~42% and pH ~ 12 (donated by Moorim P&P Company, Ulsan, South Korea) and other chemicals such as H_2SO_4, $C_2H_2O_2$, and NaOH (Duksan Chemicals, South Korea) were used. Figure **1** shows the schematic of the extraction and crosslinking of THKL. First, 4 N H_2SO_4 was dropwise added to the black liquor until a pH of 9 was reached. Second, the mixture was heated up to 70 °C and stirred for 1 h at 400 rpm. The temperature of the mixture was decreased to 40 °C, and the precipitated material was filtered using a Buchner funnel under vacuum with Whatman paper No. 1. Next, the filtered material was washed in a H_2SO_4 solution (2 wt%) at 70 °C for 1 h and filtered again using the Buchner funnel under vacuum. The precipitated lignin was washed with distilled water at 70 °C for 1 h to remove any impurities. After washing, the mixture was filtered again, and the THKL cake was dried in a 60 °C oven for 72 h. THKL crosslinking was conducted by adding 55 g of THKL and 60 g of water in a 250-mL three-necked flask equipped with a glass condenser tube, thermometer, and stirring bar. The THKL slurry was heated up to 60 ˚C, maintained constant at this temperature, and stirred for 30 min. Then, a 40% glyoxal solution was added alternately after 30 min while maintaining a constant reaction pH of ~12 using a NaOH solution at 60 ˚C for 4 h. Figure **2** shows the colors of waste kraft black liquor cake and extracted lignin powder.

2.1. FTIR Spectroscopy

Fourier-transform Infrared (FTIR) spectral measurements were performed using attenuated total reflectance–IR spectroscopy (ALPHA-P model, Bruker Optics, Germany) equipped with an ATR universal accessory at room temperature for all lignin samples. Spectra were recorded in absorbance mode with a

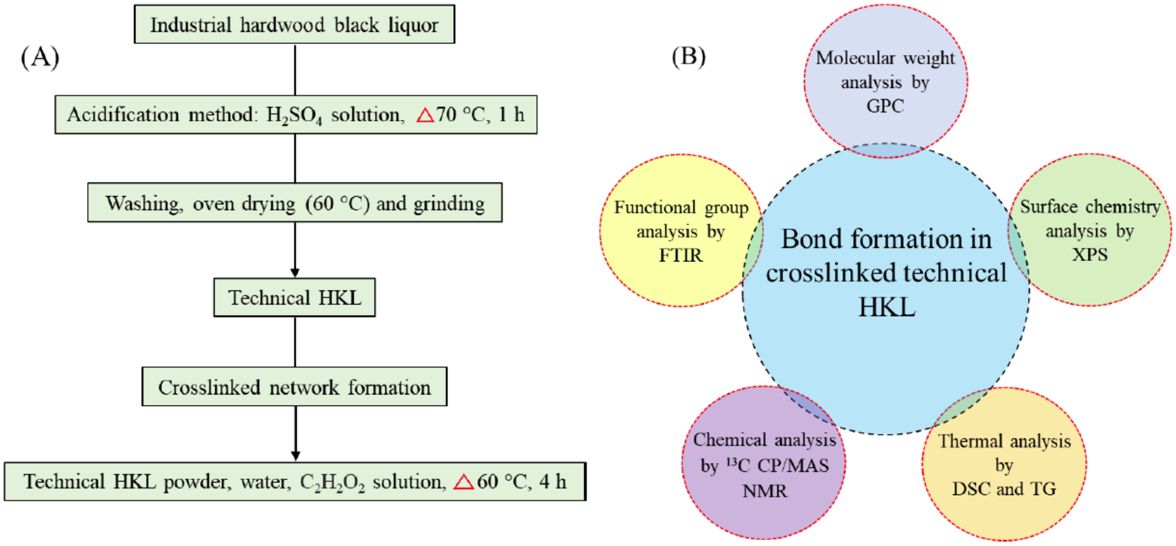

Figure 1: (**A**) THKL extraction and crosslinking and (**B**) related analyses.

scanning resolution of 4 cm^{-1} in the range of 4000–400 cm^{-1} and 64 scans for each spectrum.

2.2. Gel Permeation Chromatography (GPC)

The molecular weight and polydispersity of THKL and C-THKL were analyzed. All types of lignins, before molecular weight measurement by GPC, were acetylated with acetic anhydride in an anhydrous pyridine solvent. For GPC analysis, 2 mg of each acetylated lignin was dissolved in 1 mL of THF, sonicated for 5s, and then filtered through a 0.45 µm PTFE syringe filter. Polystyrene standards with a molecular weight of 1060-2330 kDa were used as standards. GPC measurements were performed using a Waters Alliance e2695 GPC system (Milford, MA, USA), which included a pump, an autosampler, and a column oven set at 35 °C. The GPC instrument has equipped with a refractive index (R1) detection device and run with the eluting solvent THF at a flow rate of 1 mL/min.

2.3. Solid-State ^{13}Carbon Cross-Polarization/Magic Angle Spinning Nuclear Magnetic Resonance (^{13}C CP/MAS NMR) Spectroscopy

To know about crosslinking reaction between lignin molecules by glycolic acid, solid state ^{13}C CP/MAS NMR spectra were recorded with a Bruker Avance III HD 400 instrument operating at 400 MHz. 100 mg dry lignin samples were used for the analysis. Measurements were performed at 296 ± 1 K. The MAS rate was 10 kHz. The acquisition was performed with a CP pulse sequence using a 2.95 µs proton 90° pulse, an 800 µs ramped (100%−50%) falling contact pulse, and a 2.5 s delay between repetitions.

2.4. X-Ray Photoelectron Spectroscopy (XPS)

X-ray photoelectron spectroscopy (Nexsa, Thermo Fisher Scientific, Waltham, MA, USA) was applied to determine the chemical compositions of THKL and C-THKL samples at surfaces. XPS survey scans at 80 eV and 1 eV steps were used to investigate the Na1s, O1s, N1s, C1s, and S2p regions, whereas high-resolution scans at 50 eV and 0.1 eV steps were utilized to identify specific chemical bonding of the samples using a deconvolution approach with a Gaussian function.

2.5. Deferential Scanning Calorimetry (DSC)

A DSC (Discovery 25, TA instruments, New Castle, USA) was used to determine the glass transition temperature (Tg) of the different lignin samples. The second heating cycle of DSC was done in a nitrogen atmosphere. The dried lignin sample (4 mg) was sealed in an aluminum pan with a lid. The sample was heating to 105 °C at the rate of 10 °C/min, and then isothermally conditioned for 20 min before cooling to 0 °C. The second scan were recorded by gradually increasing the temperature to 250 °C at the rate of 10 °C/min to measure Tg.

2.6. Thermogravimetry Analysis (TGA)

Thermogravimetry analysis was done by TA Instruments (Discovery SDT 650, USA). Sample sizes were 15 mg in reusable alumina crucibles with lids. The temperature program used a ramp speed of 10 °C/min and nitrogen flow of 50 mL/min and consisted of: (annealing cycle) ramp to 105 °C, isothermal 20 minutes, ramp to 30 °C, (measurement cycle) ramp to 800 °C.

3. RESULTS AND DISCUSSIONS

3.1. FTIR Analysis

Figure **3** shows the FTIR spectra of THKL with and without crosslinking (C-THKL). The broad absorption band at 3370 cm^{-1} was attributed to the aromatic and aliphatic –OH groups of THKL. The peaks at 1111 and

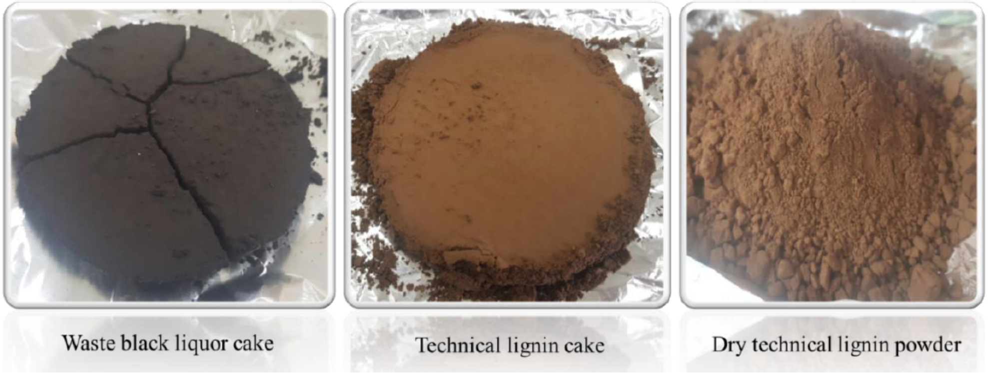

Figure 2: Color of hardwood kraft pulping black liquor waste and extracted and dried THKL.

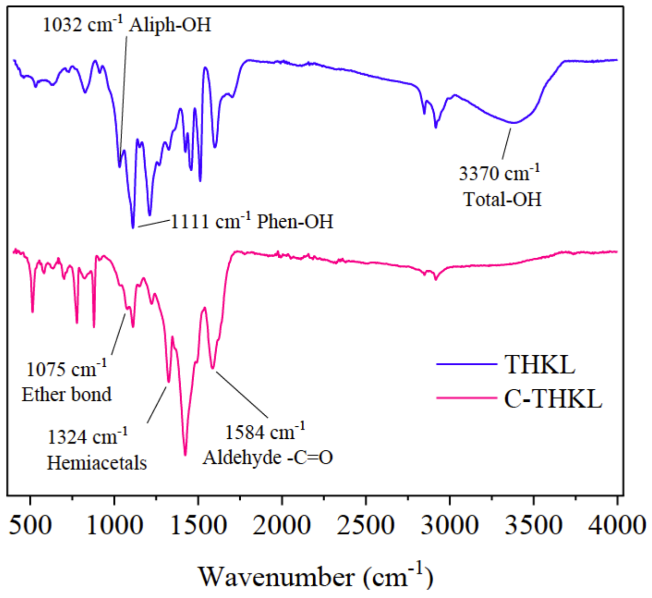

Figure 3: Chemical group changes of THKL after crosslinking.

1032 cm^{-1} corresponded to the terminal phenolic hydroxyl and side aliphatic –OH groups, respectively [6]. Scheme **1** shows the mechanism of ether bond formation using glycolic acid in THKL. By the Cannizzaro reaction of glyoxal under alkaline conditions, glycolic acid was generated, and the crosslinking of lignin occurred via the formation of ether bonds between glycolic acid and lignin functional groups. After crosslinking, significant changes were observed as indicated by different bands in the FTIR spectra. The FTIR spectrum of C-THKL showed a new peak corresponding to the R–C=O group of glyoxal and glycolic acid at 1584 cm^{-1}, which resulted from the introduction of glycolic acid into the lignin structure via the formed ether bonds. Another new peak at 1075 cm^{-1} indicated that glycolic acid reacted well with the phenolic and aliphatic carbon atoms in the lignin units [7, 8, 9]. These results revealed that the reactions between different –OH groups in THKL and glycolic acid led to the formation of ether bonds. Consequently, the R–C=O peak intensity increased, while the –OH group peak intensities (3370, 1111, and 1032 cm^{-1}) decreased in crosslinked lignin.

In addition, glycolic acid generated by the Cannizzaro reaction led to the decrease in the pH and created acidic conditions. Under these conditions, the acetalization of glyoxal occurred, affording hemiacetals via the nucleophilic reaction of an alcohol molecule (lignin alcoholic –OH) with a carbonyl cation of glycolic acid (Scheme **2**). Next, the formed hemiacetals induced the etherification of the –OH group of glyoxal,

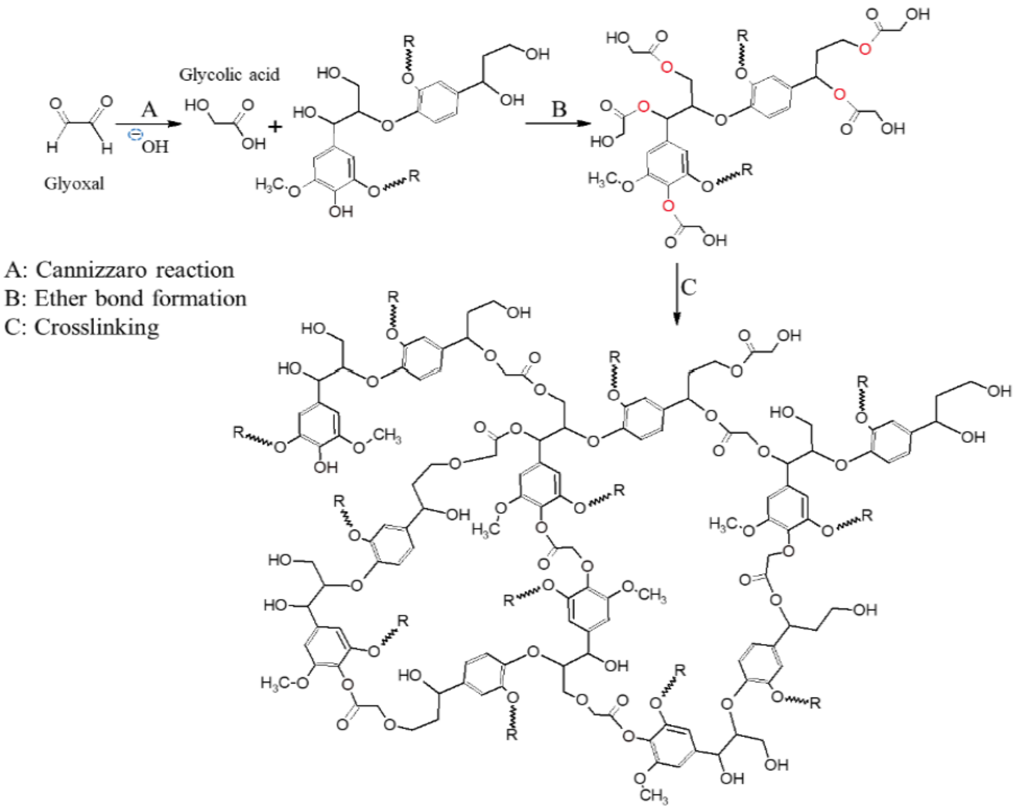

Scheme 1: Mechanism of ether bond formation by glycolic acid in THKL.

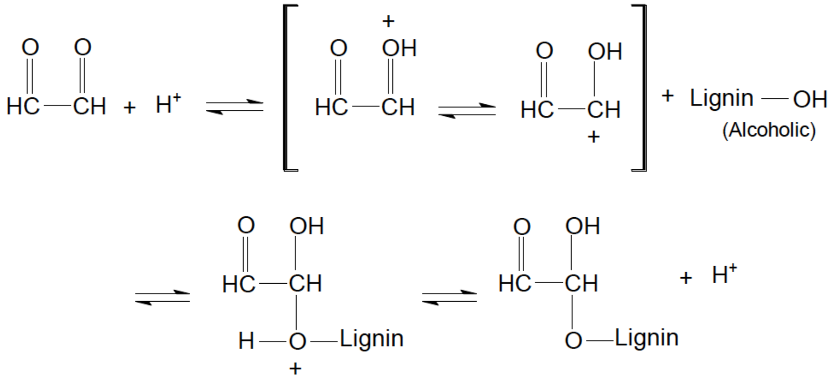

Scheme 2: Crosslinking mechanism of THKL under acidic conditions.

generating ether bonds between lignin units. The band corresponding to the C–O stretching of hemiacetals was observed at approximately 1324 cm^{-1} (Figure **3**), attributed to the acetal groups formed by crosslinking.

3.2. GPC Analysis of Molecular Weight

Figure **4** shows the molecular-weight distributions of THKL and C-THKL obtained by GPC. The molecular weight of the THKL sample increased after glyoxalation. In addition, THKL exhibited a broader molecular-weight distribution after crosslinking, indicative of the formation of larger molecules due to the new ether bonds formed between lignin molecules due to glycolic acid. Scheme **1** shows the crosslinking mechanism. Recent studies reported similar results: the molecular weight of bio-materials, such as lignin and soy protein, increased after crosslinking [10, 11, 12].

3.3. Solid-State ^{13}C CP/MAS NMR Analysis

Table **1** shows the chemical changes observed in THKL and C-THKL analyzed by solid-state ^{13}C CP/MAS NMR spectroscopy. Specific chemical shifts corresponding to C–H (32–34 ppm), aliphatic C–O (74.2 ppm), and aromatic C–O (147.3 ppm) in THKL were detected. The CP/MAS ^{13}C NMR results of C-THKL revealed that the lignin structure was altered after crosslinking. The peak intensities corresponding to the aromatic and aliphatic C–O bonds (phenolic and aliphatic –OH) decreased after crosslinking. Previous studies reported similar changes in lignin characteristics [13, 14]. The reduced peak intensities of the aromatic and aliphatic –OH groups and the appearance of new peaks (at 62–64 ppm and 168–191 ppm) due to crosslinking (as observed in FTIR spectra) were confirmed by ^{13}C NMR. Furthermore, after crosslinking, the peak intensity of the C–H bonds slightly increased due to the introduction of glycolic acid into the lignin structure [14].

3.4. XPS Analysis

Figure **5** and Table **2** show the XPS analysis results of the THKL and C-THKL samples. According to the peak positions, higher atomic percentages of C, O, N, S, and Na were observed in the lignin sample. The amount of elemental impurities was less than that obtained in other pulping methods.

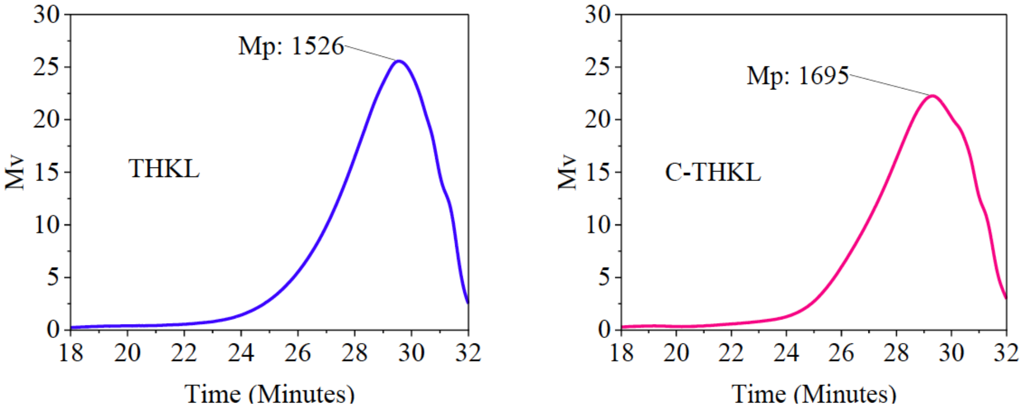

Figure 4: Molecular-weight distributions of THKL and C-THKL.

Table 1: Changes in the Peak Intensities of the ^{13}C NMR Spectra of THKL after Crosslinking

	THKL	C-THKL
NMR spectra	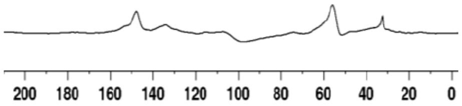	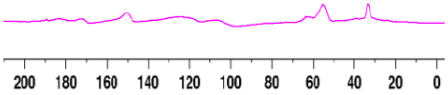
C–H bonds (32–34 ppm)	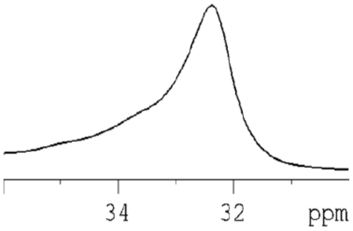	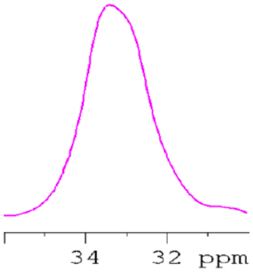
Aliphatic C–OH (74 ppm)	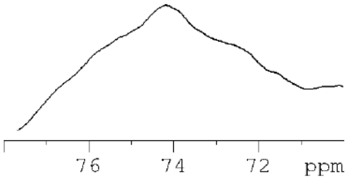	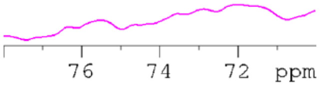
Phenolic C–OH (147.3 ppm)	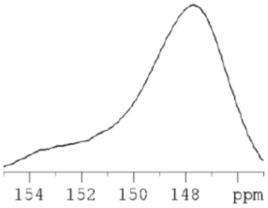	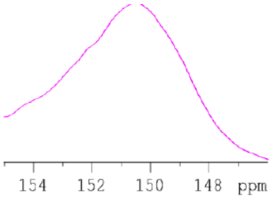
New peak Ether bond formation (62–64 ppm)		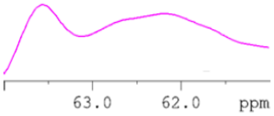
New peaks Ether bond formation (168–191 ppm)		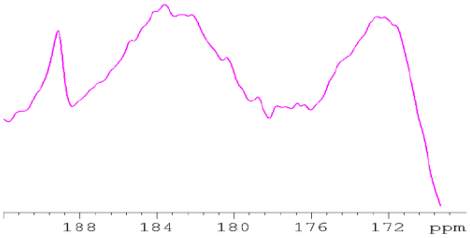

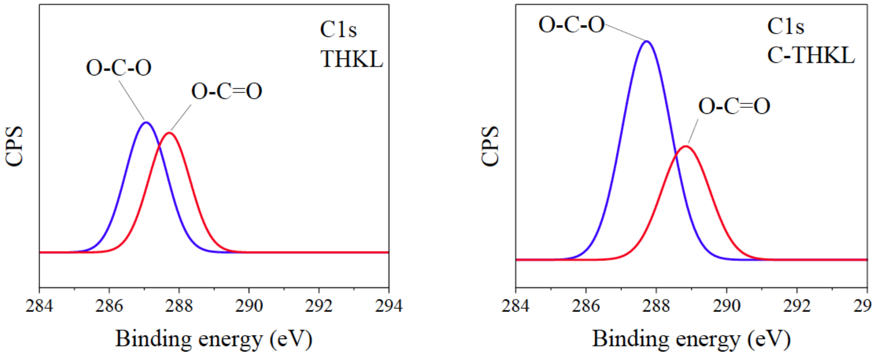

Figure 5: High-resolution XPS C1s spectra of THKL and C-THKL.

Table 2: XPS Analysis Results of THKL before and after Crosslinking

Materials	Elements	Peak Position (eV)	FWHM (eV)	Area (P)	Atomic content (%)
THKL	C1s	284.41	2.11	92901.64	83.29
	O1s	532.54	2.02	40097.46	14.88
	N1s	398.45	1.81	1448.15	0.84
	Na1s	1070.45	1.78	931.77	0.17
	S2p	167.84	2.17	1845	0.82
C-THKL	C1s	287.59	3.37	58425.61	54.71
	O1s	533.96	3.64	81991.51	31.76
	N1s	402.04	0.66	855.44	0.52
	Na1s	1073.71	2.96	65732.57	12.65
	S2p	171.49	0.18	797.4	0.37

FWHM: full width at half maximum.

Based on the obtained results, during THKL crosslinking, ether bonds were formed as indicated by the increased intensities of the peaks at 287.7 and 288.8, corresponding to O–C–O and O–C=O, respectively (Figure **6**). Furthermore, the oxygen content of C-THKL also increased from 14.88% to 31.76% due to ether bond formation. The area corresponding to O 1s increased by about two times in C-THKL. In addition, the full width at half maximum (FWHM) index for oxygen was increased by around 1.8 times, indicative of the chemical state changes during the reaction, and the broadening of the oxygen peak indicated a change in the number of the chemical bonds contributing to the peak shape.

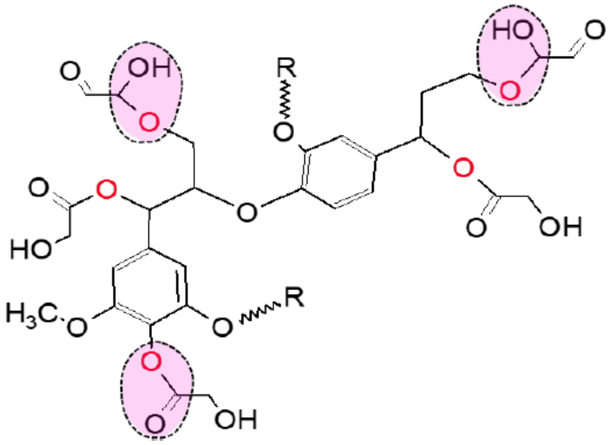

Figure 6: O–C–O bond detected by XPS.

3.5. DSC and TGA Characterization

Figure **7a** and Table **3** show the DSC results of THKL and C-THKL. The crosslinking reaction led to a change in the thermal behavior of C-THKL. When the THKL sample was heated from 0 °C to 250 °C, two transition points were observed at 70 °C and 146 °C, attributed to the impurities or other ingredients in THKL [15] and its glass temperature (T_g), respectively [16, 17, 18]. From the DSC results, the T_g of C-THKL was less than that of noncrosslinked THKL. The results also revealed that the crosslinking reaction led to an exothermic trend in C-THKL, indicative of new bond formation.

The thermal degradation behavior and weight loss of THKL and C-THKL were evaluated by TGA. Figure **7b** and **c** shows the TGA and derivative thermal gravimetry (DTG) curves of THKL and C-THKL. The TGA results revealed that crosslinking caused a lower thermal weight loss in C-THKL due to the formation of crosslinked networks. Moreover, Figure **7c** shows the comparison of different DTG curves of THKL and C-THKL. C-THKL exhibited thermal stability and a slow weight loss rate at approximately 200 °C. Noncrosslinked lignin exhibited lower thermal stability as well as char content (material retained at the end of the TG test) at 800 °C. The thermal degradation of THKL occurred at two temperature regions: less than 200 °C and between 200 °C and 800 °C. By contrast, the thermal degradation of C-THKL occurred at four temperature regions. The total weight loss percentages of THKL and C-THKL at the end of the TGA test were 64.5% and 27.7%, respectively (Table **3**). This result indicated that the crosslinking of THKL by glycolic acid led to a slow degradation rate and a lower weight loss in C-THKL. Similar result refereeing higher thermal stability due to lignin crosslinking was reported [19]. The thermal degradation at temperatures of less than 200 °C was mainly attributed to the decomposition of

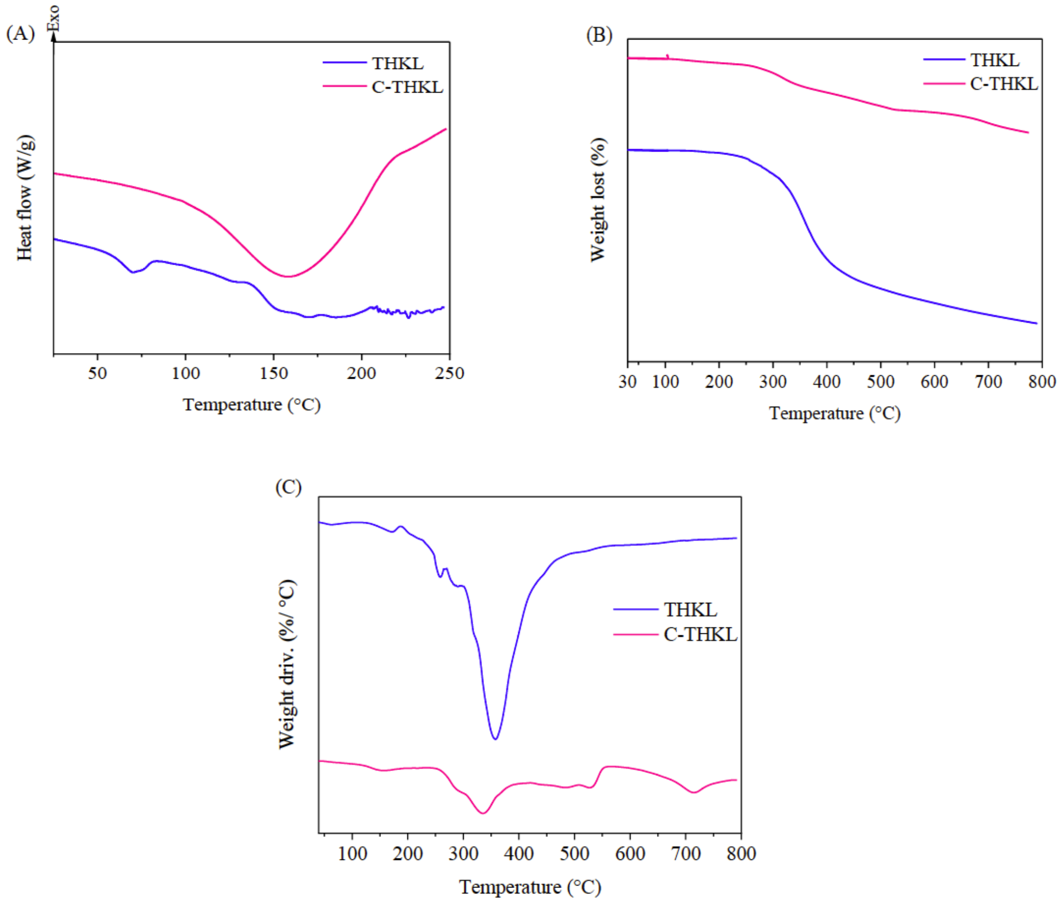

Figure 7: Thermal properties of THKL before and after crosslinking: (**A**) DSC, (**B**) TGA, and (**C**) DTG.

other chemicals, such as water, glyoxal, other phenolic compound, and impurities [9, 20].

Table 3: Thermal Behavior of THKL before and after Crosslinking

Property	THKL	C-THKL
Glass transition temperature (°C)	146	132
Weight loss (%)	64.5	27.7
Retained material (%)	35.5	72.3

4. CONCLUSION

This study investigated the potential of value-added THKL for application for bio-based adhesives. THKL was extracted from waste industrial kraft black liquor. To enhance adhesion properties, THKL was crosslinked using glycolic acid. The results revealed the successful formation of crosslinked networks in THKL. Ether bond formation between glycolic acid and the lignin functional groups was confirmed by the new peaks in FTIR and ^{13}C C/MAS NMR spectra. GPC analysis revealed an increase in the molecular weight and molecular-weight distribution of C-THKL, resulting from the bond formation. An increase in the atomic oxygen percentage and O–C–O and O–C=O count per surface versus binding energy observed by XPS confirmed ether bond formation. Thermal analysis of C-THKL revealed its exothermic behavior, lower thermal degradation rate, and higher thermal stability. Considering the amount of kraft black liquor generated by wood pulp industries and the chemical properties of THKL, THKL demonstrates promise as a raw material for the production of green, sustainable bio-adhesives via the crosslinking of its hydroxyl groups using glycolic acid.

ACKNOWLEDGEMENTS

This work was supported by the Brain Pool program of the National Research Foundation (NRF) of Korea (Grant No. 2022H1D3A2A02051596) and funded by the Korean Government (MSIT) (Grant No. RS-2023-00240043)

DECLARATION OF CONFLICTING INTEREST

The authors declare competing financial interest.

REFERENCES

[1] Suota MJ, da Silva TA, Zawadzki SF, Sassaki GL, Hansel FA, Paleologou M, Ramos LP. Chemical and Structural Characterization of Hardwood and Softwood Lignoforce™ Lignins. Ind Crops and Prod 2021; 173: 114138. https://doi.org/10.1016/j.indcrop.2021.114138

[2] Lawoko M, Samec JSM. Kraft lignin valorization: Biofuels and thermoset materials in focus. Curr Opin Green Sustain Chem 2023; 40: 100738. https://doi.org/10.1016/j.cogsc.2022.100738

[3] Giummarella N, Lindén PA, Areskogh D, Lawoko M. Fractional Profiling of Kraft Lignin Structure: Unravelling Insights on Lignin Reaction Mechanisms. ACS Sustain Chem Eng 2020; 8: 1112-1120. http://dx.doi.org/10.1021/acssuschemeng.9b06027

[4] Crestini C, Lange H, Sette M, Argyropoulos DS. On the Structure of Softwood Kraft Lignin. Green Chem 2017; 19: 4104-4121. https://doi.org/10.1039/C7GC01812F

[5] Van Nieuwenhove I, Renders T, Lauwaert J, De Roo T, De Clercq J, Verberckmoes A. Biobased Resins Using Lignin and Glyoxal. ACS Sustain Chem Eng 2020; 8: 18789-18809. https://doi.org/10.1021/acssuschemeng.0c07227

[6] Zheng L, Tao L, Li Y, Zhang X, Xu Y, Li J, Gao Q. Performance of soybean protein adhesive cross-linked by lignin and cuprum. J Clean Prod 2022; 366: 132906. https://doi.org/10.1016/j.jclepro.2022.132906

[7] Ding C, Li N, Chen Z, Zhang Y. Preparation of highly water-resistant wood adhesives using ECH as a crosslinking agent. e-polymers 2022; 22:99-107. https://doi.org/10.1515/epoly-2022-0010

[8] De Hoyos-Martínez PL, Robles E, Khoukh A, Charrier-El Bouhtoury F, Labidi J. Formulation of Multifunctional Materials Based on the Reaction of Glyoxalated Lignins and a Nanoclay/Nanosilicate. Biomacromolecules 2019; 20: 3535-3546. https://doi.org/10.1021/acs.biomac.9b00799

[9] Ammar M, Khiari R, Belgacem MN, Elalou E. Thermal characterization and comparisons of lignin-formaldehyde and lignin-glyoxal adhesives. Mediterr J Chem 2014; 2: 731-737. http://dx.doi.org/10.13171/mjc.2.6.2014.20.03.11

[10] Roy R, Jadhav B, Rahman MDS, Raynie DE. Characterization of residue from catalytic hydrothermal depolymerization of lignin. CRGSC 2021; 4: 100052. https://doi.org/10.1016/j.crgsc.2020.100052

[11] Sequeiros A, Serrano L, Briones R, Labidi L. Lignin Liquefaction Under Microwave Heating. J Appl Polym Sci 2013; 130: 3292-3298. https://doi.org/10.1002/app.39577

[12] Zhang Y, Zhu W, Lu Y, Gao Z, Gu J. Nano-scale blocking mechanism of MMT and its effects on the properties of polyisocyanate-modified soybean protein adhesive. Ind Crops Prod 2014; 57: 35-42. https://doi.org/10.1016/j.indcrop.2014.03.027

[13] Ribca I, Jawerth ME, Brett JC, Lawoko M, Schwartzkopf M, Chumakov A, Roth SV, Johansson M. Exploring the Effects of Different Cross-Linkers on Lignin-Based Thermoset Properties and Morphologies. ACS Sustain Chem Eng 2021; 9: 1692-1702. https://doi.org/10.1021/acssuschemeng.0c07580

[14] Navarrete P, Pizzi A, Pasch H, Delmotte L. Study on Lignin-Glyoxal Reaction by MALDI-TOF and CP-MAS13C-NMR. J Adhes Sci Technol 2012; 26: 1069-1082. https://doi.org/10.1163/016942410X550030

[15] Wibowo ES, Park BD. The Role of Acetone-Fractionated Kraft Lignin Molecular Structure on Surface Adhesion to Formaldehyde-Based Resins. Int J Biol Macromol 2023; 225: 1449-1461. https://doi.org/10.1016/j.ijbiomac.2022.11.202

[16] Lisperguer J, Perez P, Urizar S. Structure and Thermal Properties of Lignins: Characterization by Infrared Spectroscopy and Differential Scanning Calorimetry. J Chil Chem Soc 2009; 54: 460-463. http://dx.doi.org/10.4067/S0717-97072009000400030

[17] Gordobil O, Egüés I, Llano-Ponte R, Labidi J. Physicochemical Properties of PLA Lignin Blends. Polym Degrad Stab 2014; 108: 330-338. https://doi.org/10.1016/j.polymdegradstab.2014.01.002

[18] Assumpção NRL, Lona LMF. Effect of Lignin without Surface Treatment in In Situ Methyl Methacrylate Miniemulsion Polymerization. ACS Sustain Chem Eng 2022; 10: 3219-3226. https://doi.org/10.1021/acssuschemeng.1c07467

[19] Zhen X, Cui X, Al-Haimi AANM, Wang X, Liang H, Xu Z, Wang Z. Fully bio-based epoxy resins from lignin and epoxidized soybean oil: Rigid-flexible, tunable properties and high lignin content. Int J Biol Macromol 2024; 254: 127760. https://doi.org/10.1016/j.ijbiomac.2023.127760

[20] Khan MA, Ashraf SM. Studies on Thermal Characterization of Lignin Substituted Phenol Formaldehyde Resin as Wood Adhesives. J Therm Anal 2007; 89: 993–1000. https://doi.org/10.1007/s10973-004-6844-4

Received on 15-09-2023 Accepted on 16-10-2023 Published on 20-11-2023

https://doi.org/10.6000/1929-5995.2023.12.14